LBL-19883
Preprint c.2

Lawrence Berkeley Laboratory

UNIVERSITY OF CALIFORNIA

RECEIVED
LAWRENCE
BERKELEY LABORATORY
JUL 24 1985
LIBRARY AND
DOCUMENTS SECTION

Materials & Molecular Research Division

Submitted to Comments on Condensed Matter Physics

STUDIES OF THERMALIZATION OF EXCITONS
BY TIME-RESOLVED PHOTOLUMINESCENCE

P.Y. Yu

July 1985

TWO-WEEK LOAN COPY
This is a Library Circulating Copy
which may be borrowed for two weeks.

LBL-19883 c.2

Prepared for the U.S. Department of Energy under Contract DE-AC03-76SF00098

DISCLAIMER

This document was prepared as an account of work sponsored by the United States Government. While this document is believed to contain correct information, neither the United States Government nor any agency thereof, nor the Regents of the University of California, nor any of their employees, makes any warranty, express or implied, or assumes any legal responsibility for the accuracy, completeness, or usefulness of any information, apparatus, product, or process disclosed, or represents that its use would not infringe privately owned rights. Reference herein to any specific commercial product, process, or service by its trade name, trademark, manufacturer, or otherwise, does not necessarily constitute or imply its endorsement, recommendation, or favoring by the United States Government or any agency thereof, or the Regents of the University of California. The views and opinions of authors expressed herein do not necessarily state or reflect those of the United States Government or any agency thereof or the Regents of the University of California.

To Appear in Comments on
Condensed Matter Physics

LBL- 19883

STUDIES OF THERMALIZATION OF EXCITONS BY TIME-RESOLVED PHOTOLUMINESCENCE

Peter Y. Yu
Department of Physics
University of California, Berkeley
and
Materials & Molecular Research Division
Lawrence Berkeley Laboratory
Berkeley, California 94720

Abstract

Recent experimental results in the application of time-resolved photoluminescence to study the thermalization of excitons in semiconductors such as Cu_2O, AgBr and CdS are discussed. It is shown that such studies provided detailed information on the interaction between excitons and phonons and on how these interactions affect the thermalization of excitons and exciton-polaritons.

Introduction

In this Comment, the word thermalization will mean processes by which a system achieves thermal equilibrium. The system I am interested in consists of electrons and holes in semiconductors which have been produced by illumination with either a continuous wave (cw) or a pulsed radiation source. What has been called thermal equilibrium in such systems is really a steady state in which the photoexcited carriers have distributions that can be approximated by equilibrium distributions. For example, uncorrelated electrons and holes usually relax via electron-phonon interactions to band extrema where their distributions are both given by Fermi-Dirac distributions with a quasi-Fermi level for the electrons and one for the holes. If the electrons and holes are attracted by Coulomb interaction, they form correlated pairs or excitons which are bosons. The excitons behave like neutral free particles, and they relax into a distribution which can be approximated by the Boltzmann distribution. In this article, I will be concerned only with correlated electron-hole pairs.

In a typical cw photoluminescence experiment, one excites excitons with a narrow energy distribution by means of a laser. In most cases, the excitons relax by exciton-phonon interaction in a time which is short compared to the exciton radiative lifetime. Thus, the emission spectra reflects the thermalized distribution of the exciton and contains no information on the intermediate thermalization process. By assuming that the excitons follow a Maxwell-Boltzmann distribution, one can analyze the emission spectra to determine the effective temperature of the exciton in quasi-thermal equilibrium with the lattice. In principle, one can learn a lot about the thermalization processes

if one can measure the exciton emission before they become thermalized. There are at least two ways to measure such nonthermalized luminescence (sometimes referred to as hot luminescence in the literature). In the first way, one shortens the exciton lifetime so that the exciton thermalization time is now longer than or comparable to its lifetime. In this case, the emission can be excited by a cw source. In the second method, one uses a pulsed source with a pulse length which is short compared to the thermalization time to excite the emission which is then detected with a time-resolved technique.

So far, nonthermalized emission has been measured mostly with the first method. Interestingly enough, they have been observed both in samples of poor quality[1-3] and in samples with extremely high quality.[4-7] In poor samples, the exciton lifetimes are shortened by nonradiative recombination at defects. On the other hand, in samples with electric dipole-active excitons, nonthermalized emission lineshapes have been reported only in high quality samples at low temperatures. In these materials, the reason why the emission is nonthermalized is rather interesting.

It is well known that electric-dipole active excitons which are not strongly damped form coupled photon-exciton modes known as exciton-polaritons (to be abbreviated as polaritons). Outside the sample, the polaritons are just ordinary photons. Inside the sample, the polaritons are photons 'dressed' by excitons (analogous to a polaron which is an electron 'dressed' by phonons). Thus the thermalization of polaritons inside the crystal is equivalent to a radiation field coming into thermal equilibrium with a cavity. Since the incoming photons have energies of the order of an electron volt while the sample temperature is typically $\leq 100^{\circ}$ K, the polaritons have to suffer many inelastic collisions (basically Raman and Brillouin scatterings) in order to equilibrate with the lattice. For this to occur the lifetime of the

polariton inside the sample must be long compared to the scattering time. Since this lifetime is usually very small when the polariton is photon-like the polaritons do not equilibrate with the lattice. Another way to approach this problem is to consider the dispersion curves of polaritons as compared with those of excitons. Bare excitons (i.e., not coupled to photons) have dispersion curves similar to free particles so they can equilibrate with the lattice just like a collection of atoms or molecules will equilibrate with a container which acts as a heat bath. However, the dispersion curve of a polariton is quite different from that of a free particle (a schematic diagram comparing the dispersion curves of polaritons, bare excitons and photons is shown in Fig. 1). Since the minimum energy of a polariton is zero, in principle polaritons have to thermalize into the zero energy state. When the polariton energy is small, it is basically a photon so it will interact only very weakly with the lattice. As a result, one concludes again that the polariton will not come into thermal equilibrium with the lattice. However, Toyozawa[8] pointed out that polariton lifetime has a maximum around the exciton energy and he labelled it as the 'polariton bottleneck.' If the interaction time between the polaritons and phonons is short compared with the polariton lifetime at the bottleneck, then it is possible for the polaritons to thermalize around the bottleneck. Thus, whether polaritons can reach a quasi-thermal equilibrium or not depends on these two times: the polariton-phonon scattering time which is determined mainly by the exciton part of the polariton and the polariton lifetime inside the sample which is determined either by the trapping of polaritons at defects or by its escape from the sample via its photon part.

Although nonthermalized emission spectra obtained under cw excitation conditions have been around for some time, they are difficult to analyze because these spectra are typically broad and featureless.[9,10] Recently,

nonthermalized emission spectra have been obtained by pulsed excitation with picosecond lasers. These spectra contain considerably more information since the spectra lineshape changes with time. For the first time, it has been possible to extract detailed information about the thermalization of excitons and of polaritons from the time-resolved nonthermalized emission spectra. The materials which have been studied include Cu_2O, AgBr, CdS and CdSe. The former two materials are ideal for studying the behavior of excitons since the excitons are not strongly coupled to photons, while CdS and CdSe are classic materials for studying polaritons. Since these time-resolved measurements are possible recently mainly because of advances in techniques for the generation of very short laser pulses, I have included a brief discussion of the experimental techniques in the Appendix.

Theory

Calculation of nonthermalized luminescence lineshapes can now be performed even with microcomputers. Typically, it involves solving numerically a rate equation for the carrier population $\rho(E)$ in the form of:[9]

$$\frac{d\rho(E)}{dt} = G(E) - S(E) - \frac{\rho(E)}{\tau_l} \qquad [1]$$

Where E is the energy of the carrier, G(E) is the generation rate due to the laser and scattering of carriers from other energies into the state E, S(E) is the scattering rate due to carrier-phonon, carrier-carrier interactions and τ_l is the carrier population lifetime due to radiative and non-radiative recombinations. Most of the physics is contained in the calculation of S(E). In the cases of interest to us, the photoexcited carrier densities are low enough that carrier-carrier interactions can be neglected. Then S(E) is determined by electron-acoustic phonon and electron-optic phonon interactions. In general, these interactions are responsible for the thermalization of the carriers. We also note that the electron-phonon interactions do not decrease the total carrier population; they only redistribute the population. On the other hand, processes contributing to τ_l deplete the overall carrier population.

If we can define a mean electron-phonon scattering time τ_{e-p}, then it is obvious that whether the steady state luminescence is thermalized or not depends on the relative magnitude of τ_{e-p} and τ_l. For $\tau_{e-p} \ll \tau_l$, the carriers can reach thermal equilibrium before recombination so the emission has a thermal equilibrium lineshape. When $\tau_{e-p} > \tau_l$, then the

emission is nonthermalized. In actual cases, this simple picture may be complicated by the fact that both τ_{e-p} and τ_1 can be energy-dependent. In principle, by analyzing the nonthermalized emission lineshape and its time-dependence one can measure directly τ_1 and τ_{e-p} as a function of energy.

The simple Equation [1] is not valid at high carrier densities. It has been found that for carrier densities typically above 10^{18} cm^{-3}, the electron-LO phonon can be screened and the energy gaps are renormalized.[11] These effects cause τ_{e-p} and the density-of-states to be density dependent. At still higher densities, Auger processes become dominant and τ_1 becomes density dependent also.[12] Another complication to Eq. [1] arises when the electron relaxation generates so many phonons that the phonon population becomes time-dependent. When this happens, it is necessary to write down another rate equation for the phonon population and solve both the electron and phonon rate equations simultaneously. So far there have been reports of TRPL experiments in these high carrier density regimes[13] but most of them have not been analyzed quantitatively because of the complications discussed above. Therefore, in this Comment I will concentrate more on the recent low excitation experiments.

Theoretically, one can solve Eq. [1] and display the results in two ways. One can plot $\rho(E)$ versus t for various energies E or plot $\rho(E)$ versus E for various times t. Experimentally, it is usually more convenient to measure $\rho(E)$ as a function of time for different energies. So it is important to interpret the experimental $\rho(E)$ versus time curves correctly.

Let us assume the population ρ at energy E is given by a simple equation of the form:

$$\frac{d\rho}{dt} = G(t) - b\rho \qquad [2]$$

where $G(t)$ is the rate of generation and $b\rho$ is the decay rate. The solution of Eq. [2] can be written as:

$$\rho(t) = e^{-bt} \int_{-\infty}^{t} G(t)\, e^{bt} dt \qquad [3]$$

assuming the initial condition to be $\rho(-\infty) = 0$. It is generally assumed that $G(t)$ is a delta function $A\delta(t)$ so that $\rho(t) = AG(o)\, e^{-bt}$. Thus the population decays exponentially, and, from the gradient of the semilog plot $\ln\rho$ versus t, the decay time b^{-1} can be measured. In most solids, this is an exception rather than the norm. Even when the excitation laser pulse can be approximated by a delta function in time, the single exponential solution is valid only for the population at the energy of excitation. The populations at all other energies are built up from decay of populations in higher energy states, and therefore their generation rates are not delta functions. Let us assume that the population $\rho(E)$ is created by decay of another state whose population $\rho(E',t)$ changes as $\rho(E',t) = \rho(E',o)e^{-at}$ so $G(t)$ has the form Ae^{-at}. Substituting into Equation [3], we get

$$\rho(E,t) = \frac{A}{(b-a)} \left(e^{-at} - e^{-bt}\right) \qquad [4]$$

The important thing to note about Eq. [4] is the symmetric role of a and b. Normally we expect that the population $\rho(E,t)$ will show a rise time given by a^{-1} and a decay time equal to b^{-1}. Equation [4] shows that this is true only when $a \gg b$. When the reverse is true, the rise time of ρ is determined by b^{-1} while its decay time is equal to a^{-1}! In both cases, the time dependence of ρ is not exponential except for time large compared to both a^{-1} and b^{-1}.

In solids there are usually continua of electronic states, and carriers in these states can scatter into each other via phonons. In principle, the populations $\rho(E,t)$ are solutions of many coupled rate equations, and one should not expect a simple exponential decay for $\rho(E,t)$. However, in most cases the electron-phonon scattering time τ_{e-p} is much shorter than the carrier lifetime τ_1. Only for time $\lesssim \tau_{e-p}$ are the decays of $\rho(E,t)$ non-exponential. For $t \gg \tau_{e-p}$, the entire carrier distribution will be in thermal equilibrium, so $\rho(E,t)$ decays exponentially with the same time constant τ_1 independent of energy E. From this discussion, it is clear that by measuring the photoexcited carrier distribution as a function of time, one can determine, first, the time for the carriers to reach thermal equilibrium (equilibration time). This time is mainly determined by τ_{e-p}. Secondly, one can determine the lifetime (τ_1) of the thermalized population.

Recent Experimental Results

Since this Comment is not meant to be a review article, no attempts will be made to include here all the available experimental results on TRPL. Nor will time-resolved experiments in which lineshapes are already thermalized be considered, since this discussion is aimed at understanding nonthermalized emission lineshapes. Experiments will be divided into two categories. In

the first category the excited carriers form excitons, but not polaritons, because the excitons are either indirect or electric-dipole forbidden. In the second category, the excitons have strong dipole moments and form exciton-polaritons.

a. Thermalization of Excitons

From the theoretical point of view, the thermalization process of excitons is relatively well understood. Excitons relax by scattering with optical phonons (OP) and acoustic phonons (AP). Suppose at $t = 0$ a narrow distribution of excitons is created at energy $E_o >> E_x$ (minimum exciton energy) as shown in Fig. 2. In typically less than 1 ps, excitons will relax to the band bottom by emission of OP. Then the excitons thermalize by scattering with AP. The equilibration time varies from picoseconds to nanoseconds depending on the lattice temperature. After the excitons have reached thermal equilibrium, their population distribution is given by the Maxwell-Boltzmann distribution:

$$\rho(E) \propto \sqrt{E-E_x} \exp\left[-(E-E_x)/k_B T\right] \qquad [5]$$

This exciton distribution can be determined from the exciton luminescence. Because of momentum conservation, the zero-phonon exciton recombination peak reflects only the population of excitons with small momentum. To determine the exciton population at larger momentum, it is necessary to study the phonon-assisted recombination peaks.

In Fig. 3(a) is an example of a fit to the phonon-assisted exciton luminescence peaks in Cu_2O with Eq. [5]. From such fits, one can determine the exciton temperature and phonon energies, but no details of the exciton-phonon scattering process.

Recently, experimental studies of TRPL have been reported by Weiner et al.[14-16] in Cu_2O and by Stolz et al.[17,18] in AgBr. These authors have determined directly τ_{e-ph} by exciting resonantly in their sample a delta-function-like distribution of excitons with picosecond dye laser pulses. The excitation processes are shown schematically by arrows 1 and 2 in Fig. 4. A phonon is emitted in the excitation process in order that excitons with non-zero momentum are created. The exciton energy (E_x) is determined by the equation: $E_x = \hbar\omega_i - \hbar\omega_{ph}$ where $\hbar\omega_i$ is the incident photon energy, and $\hbar\omega_{ph}$ is the phonon energy. To determine the decay time of the exciton population at E_x due to exciton-phonon scattering, the emission at photon energy $\hbar\omega_s = E_x - \hbar\omega_{ph}$ is monitored. The emission process is shown in Fig. 4 by arrows 3 and 4 and again a phonon is involved to conserve momentum. This is a case in which the exciton population being measured is generated directly by a delta-function pulse, so the solution to Eq. [2] should be an exponential function in time. This was found experimentally to be indeed the case.[21] In both Cu_2O and AgBr, the measured decay times τ_1 are interpreted as determined mainly by exciton-phonon scattering. Based on this interpretation both the magnitude of τ_1 and its dependence on the exciton energy are well explained by theory.[15,16] In Fig. 5 the exciton-phonon scattering rates in AgBr extracted from the experimental results are decomposed into contributions from intravalley (Γ_{ac}), intervalley

($\Gamma_{TA(X)}$ and $\Gamma_{LA(X)}$) exciton-phonon scatterings and trapping by defects (Γ_o). From this fit, the exciton-phonon deformation potentials are determined.

It is important to note that in Fig. 4 , although the excitons suffer no inelastic scattering between absorption and emission, elastic dephasing scattering can occur. The dephased component of the emission has been labelled as hot luminescence while the non-dephased component as resonant Raman scattering. It has been suggested that time-resolved measurements can be utilized to separate the two components.[19] Based on the time dependent results, Weiner and Yu[15] concluded that in Cu_2O the emission is dominated by hot luminescence.

It is well-established that the 1s orthoexciton in Cu_2O is electric-dipole forbidden, but electric-quadrupole allowed.[20] So in addition to the phonon-excitation process sketched in Fig. 4, it is possible to excite zone-center excitons directly by quadrupole absorption. It has been pointed out by Habiger and Compaan[21] that such 'cold' excitons will thermalize by first absorbing an LA phonon of frequency ~5cm^{-1} (corresponding to T ~7 K). If the sample temperature is << 7 K, the photoexcited exciton will first warm up to ~7 K before cooling back to the lattice temperature. Instead of heating the sample, the laser will actually cool the sample!

This thermalization of cold excitons in Cu_2O has been observed by TRPL by Weiner and Yu.[16] Their experimental TRPL spectra are compared with theoretically calculated spectra in Fig. 6 . The cold excitons are excited by tuning the picosecond dye laser frequency to the 1s orthoexciton frequency of 16397 cm^{-1}. The exciton distribution is determined from the Γ_{12}^--phonon assisted exciton recombination peak between 16287 and 16297 cm^{-1}. In Fig. 6(c) one sees that after ~0.5 nsec, a broad peak appears in the exciton distribution

at ~5 cm^{-1} above the exciton band minimum due to LA phonon absorption. This peak reaches its maximum intensity in ~1.6 nsec. It took the exciton about 5 nsec to reach a thermal equilibrium lineshape. The theoretical spectra shown in Fig. 6(c) and (d) reproduces all the experimental results with no adjustable parameter. This excellent agreement between theory and experiment is due to the fact that very detailed information is available on the properties of excitons in Cu_2O.

b. Thermalization of Exciton-Polaritons

When excitons are electric-dipole active, the electromagnetic wave and the exciton polarization form a coupled propagating mode known as exciton polaritons. Several reviews on polariton properties have appeared recently.[22] Here we will be concerned with the polariton thermalization process only.

The thermalization procedure for the exciton described earlier is not valid anymore because the polariton dispersion curve no longer has a minimum at the transverse exciton energy as shown in Fig. 1. In principle, the polariton can continue to relax in energy down to the zero energy state. Experimentally, however, one observes emission at photon energies close to the transverse exciton energy. Typically this polariton emission curve is much broader than predicted by Equation [5]. The polariton emission lineshape was qualitatively explained by Toyozawa[8] who pointed out that the polariton lifetime should be determined mainly by two processes.

First, polaritons relax by emission of acoustic phonons. Since only the exciton part of the polariton interact with acoustic phonons, the phonon scattering rate should decrease below the transverse exciton energy when the polariton becomes essentially photon-like. As the polariton becomes more photon-like, its group velocity increases and its probability of escaping from the crystal also increases. Figure 7 shows the calculated phonon scattering rate (dotted curve) and radiative decay rate (broken curve) as a function of polariton energy in CdS.[23] The total decay rate (solid curve) shows a minimum (or a maximum in lifetime which Toyozawa labelled the polariton bottleneck) slightly below the transverse exciton frequency (20589.5 cm^{-1}). Based on this theory, if one measures the decay time of the polariton emission as a function of polariton energy, one should see a maximum in the decay time at the polariton bottleneck.

In 1975, Wiesner and Heim[24] reported for the first time the polariton decay time as a function of energy in CdS for several temperatures. Two aspects of their results are quite interesting. Firstly, they found that the polaritons were not in thermal equilibrium at low temperatures ($T < 10^{o}K$) in agreement with Toyozawa's theory, but the decay time shows only a plateau instead of a maximum. Secondly, at higher temperatures ($T \gtrsim 25^{o}K$) the polariton distribution was in thermal equilibrium. Wiesner and Heim could interpret their result only qualitatively and still left open the question as to whether the polariton lifetime in CdS had a bottleneck.

Recently, Askary and Yu[25] repeated the experiment of Wiesner and Heim and also compared the experimental results with the results of a model calculation. They found good qualitative agreement between theory and

experiment. At low temperatures, polaritons above the bottleneck accumulate in the lower branch where they relax via emission of acoustic phonons. As a result, the polariton decay time increases with decrease in the polariton energies as predicted by Toyozawa. However, when the polariton energy is below the bottleneck, their decay time becomes shorter than the time it takes to generate them. According to Equation [4], in this region the polariton lifetime measured by Wiesner and Heim represents the generation time rather than the decay time. As a result a plateau rather than a peak is observed. Askary and Yu calculated the time-dependence of the polariton emission at different energies and extracted the polariton decay time versus polariton energy. In Figure 8, this decay time is compared with the inverse of the decay rate shown in Figure 7. From the two curves it is quite clear that the two quantities are identical only for polaritons with energy above the bottleneck. Polaritons with energy lower than the bottleneck have decay times equal to the lifetime of the bottleneck because they are populated by relaxation of polaritons from the bottleneck. At finite temperatures, the polariton-phonon scattering rate increases, while the radiative recombination rate is almost constant. At temperatures $T \geq 10^{o}K$, the scattering rate becomes fast enough for the polaritons at the bottleneck to reach a quasi-thermal equilibrium. This is shown clearly in Figure 9 where the polariton distribution functions are plotted at various time delays after impulse excitation.[26] At $T = 10^{o}K$, it takes the polariton about 5 nsec to attain quasi-thermal. This equilibration time decreases with temperature rapidly. At $T \gtrsim 25^{o}K$, the equilibration time becomes shorter than the time resolution in the

experiment of Wiesner and Heim. This explains why they found the polariton distribution to be in thermal equilibrium at 25°K. Thus the presence of the bottleneck in the polariton lifetime is crucial in understanding how the polariton distribution (and hence the polariton emission curve) varies from a nonthermal equilibrium distribution to a thermal equilibrium distribution as temperature increases.

In summary, TRPL measurement is a powerful technique for studying the dynamic behavior of excitons in condensed matter. In systems where the exciton lifetimes are long enough to reach thermal equilibrium before recombination, TRPL is complementary to steady-state PL and enables important parameters, such as exciton lifetime and electron-phonon scattering time, to be determined directly. In systems where the excitons do not reach thermal equilibrium before recombination, steady-state PL spectra often do not carry much information and TRPL results are very useful in understanding the steady-state PL spectra.

Acknowledgement

This work was supported by the Director, Office of Energy Research, Office of Basic Energy Sciences, Materials Sciences Division of the U.S. Department of Energy under Contract No. DE-AC03-76SF00098. The author gratefully acknowledges H. Stolz for preprints of their work.

Appendix: Experimental Techniques

In most semiconductors, photoexcited carriers relax via scattering with phonons. The scattering rates vary typically from ~10^{10} sec^{-1} for acoustic phonons to ~10^{13} sec^{-1} for longitudianl optical (LO) phonons.[27] Typical radiative decay rates of carriers are ~10^{9} sec^{-1} while non-radiative decay rates (due to defects) can vary from <10^{9} sec^{-1} to >10^{12} sec^{-1} depending on the sample quality.[28] Thus to study time-resolved photoluminescence (TRPL) in semiconductors, a setup capable of generating and detecting picosecond duration light pulses is needed.

The recent availability of such light sources and detectors commercially makes measurement of TRPL a routine experiment. It is not the purpose of this article to review all the available light sources and detectors suitable for TRPL, so only some commonly available systems, including their advantages as well as limitations, will be summarized here.[29]

A. Picosecond Light Sources

Although it is possible to study TRPL with incoherent light sources producing pulses of duration $\gtrsim$ 100 psec, most TRPL experiments in solids use modelocked lasers as the excitation source. Several such modelocked laser systems and their properties are summarized in Table I. These lasers have been selected because their high repetition rate makes them particularly suitable for TRPL studies. When higher peak powers are desirable, the Nd:YAG laser can be Q-switched, and the dye laser cavity-dumped to generate pulses with megawatts of peak power.

B. Detection Systems

Several detection schemes are available which offer subnanosecond time-resolution with sufficiently high sensitivity for measuring emission in samples of relatively low quantum efficiency. Some of these are summarized below:

(i) Streak Cameras[29]

In principle, the streak camera offers the best combination of versatility, time-resolution and sensitivity for TRPL experiments. The best commerically available units have time-resolution of ~1 psec and sensitivity for detecting single photons. Their only drawback is their high price.

(ii) Optical Gating

In these techniques, the laser pulses are typically split into two beams. One beam is used to excite the sample, while the other is used to "gate" the detector. With high power lasers, the laser can be used to open a Kerr shutter before the detector. In the technique pioneered by Mahr and coworkers[13] the laser is mixed with the photoluminescence in a nonlinear crystal to generate the sum frequency. By varying the delay between the laser and the photoluminescence, the temporal profile of the latter can be determined. The disadvantage of this scheme is its low sensitivity; consequently, only solids with high quantum efficiency can be studied. Furthermore, because this optical gate can sample only one emission frequency at one delay at a time, its efficiency of data accumulation is low.

(iii) Delayed Coincidence Photon Counting[28]

A schematic diagram of this detection system is shown in Figure 10. The heart of this system is the fast constant fraction discriminators (CFD) and time-to-amplitude converter (TAC). The time resolution of the electronic system is estimated to be $\lesssim$ 30 psec. In practice, the time resolution of these systems is limited by the photomultiplier tube. With more conventional photomultiplier tubes and deconvolution of spectra, decay times as short as 100 psec have been determined. With the new microchannel based photomultiplier tubes, it should be possible to measure decay times as short as ~ 30 psec. The advantages of the detection scheme are its relatively low cost, ease of operation and single-photon sensitivity. Also, with microchannel plate based photomultipliers equipped with a resistive anode,[30] it should be possible to obtain entire emission spectra as a function of time.

References

1. R. Fisher, U. Heim, F. Stern and K. Weiser, Phys. Rev. Lett. 26, 1182 (1971).

2. Y. Petroff, P. Y. Yu and Y. R. Shen, Phys. Rev. B12, 2488 (1975).

3. J. I. Pankove and D. E. Carlson, Appl. Phys. Lett. 29, 620 (1976).

4. E. Gross, S. Permogorov, V. Travnikov and A. Selkin, Solid State Commun. 10, 1071 (1972).

5. D. D. Sell, S. E. Stokowski, R. Dingle and J. V. DiLorenzo, Phys. Rev. B7, 4568 (1973).

6. H. Sumi, J. Phys. Soc. (Japan) 41, 526 (1976).

7. F. Askary and P. Y. Yu, Solid State Commun. 47, 241 (1983).

8. Y. Toyozawa, Progr. Theor. Phys. Suppl. 12, 111 (1959).

9. N. Caswell, J. W. Weiner and P. Y. Yu, Solid State Commun. 40, 843 (1981).

10. V. V. Travnikov and V. V. Krivolapchuk, JETP Lett. 36, 243 (1982).

11. See for example K. Kash and J. Shah, Appl. Phys. Lett. 45, 401 (1984) and references therein.

12. See for example E. Wintner and E.P. Ippen, Appl. Phys. Lett. 44,999 (1984) and references therein.

13. See T.P. Daly and H. Mahr, Phys. Rev. B29, 5591 (1984) and references therein.

14. J.S. Weiner, N. Caswell, P.Y. Yu and A. Mysyrowicz, Solid State Commun. 46, 105 (1983).

15. J.S. Weiner and P.Y. Yu, Solid State Commun. 50, 493 (1984).

16. J.S. Weiner and P.Y. Yu in Proceedings of the XVII International Conference on the Physics of Semiconductors, ed. by J.D. Chadi and W.A. Harrison (Springer-Verlag, New York, 1985) p.1207.

17. H. Stolz and W. von der Osten, Solid State Commun. 49, 1035 (1984).

18. H. Stolz, E. Schreiber and W. von der Osten in Proceedings of the XVII International Conf. on the Physics of Semiconductors, ed. by J.D. Chadi and W.A. Harrison (Springer-Verlag, New York, 1985) p.1271.

19. Y.R. Shen, Phys. Rev. B9, 622 (1974).

20. See for example S. Nikitine in Optical Properties of Solids, eds. S. Nadelman and S.S. Mitra, Plenum, New York (1969).

21. R.M. Habiger and A. Compaan, Solid State Commun. 18, 1531 (1976).

22. See for example articles by P.Y. Yu in Light Scattering in Solids, eds. J.L.Birman, H.Z. Cummins, and K.K. Rebane, Plenum, New York (1979) p. 143; E.S. Koteles in Excitons, eds. E.I. Rashba and M.D. Sturge, North Holland, Amsterdam (1982) p. 83; R.B. Ulbrich and C. Weisbuch in Festkorperprobleme (Advances in Solid State Physics) ed. J. Treusch, Vieweg, Braunschweig (1978), Vol. XVIII, p. 217; and C. Weisbuch and R. Ulbrich in Light Scattering in Solids III, Topics in Applied Physics, Vol. 51, eds. M. Cardona and G. Guntherodt, Springer, New York (1982).

23. Farid Askary, Ph.D. Thesis, University of California, Berkeley, Berkeley, California (unpublished, 1983).

24. P. Wiesner and U. Heim, Phys. Rev. B11, 3071 (1975).

25. F. Askary and P.Y. Yu, Phys. Rev. B28, 6165 (1983).

26. F. Askary and P.Y. Yu, Phys. Rev. B31, 6643 (1985).

27. See for example E.M. Conwell and M.O. Vassel, IEEE-ED 13,22 (1966).

28. See for example J.S. Weiner and P.Y. Yu, J. Appl. Phys. 55, 3889 (1984).

29. See for example articles in Ultrashort Light Pulses - Picosecond Technique and Applications (Topics in Applied Physics, Volume 18), ed. by S.L. Shapiro (Springer-Verlag, New York, 1977).

30. See for example C. Firmani, E. Ruiz, C.W. Carlson, M. Lampton and F. Paresce, Rev. Sci. Inst. 53, 570 (1982).

TABLE 1 A comparison between a few common sources of picosecond laser pulses for time-resolved photoluminescence studies

	Laser	Pulse Duration	Photon Energy	Repetition Rate	Energy/ Pulse
(a)	Modelocked cw Nd:YAG	< 100psec	1.17 eV or 2.34 eV	~10^8Hz	≲100nJ
(b)	Modelocked cw Ar^+	~200psec	2.4-2.7 eV in discrete steps	~10^8Hz	~10nJ
(c)	Dye Laser Pumped by modelocked cw Nd:YAG	≳1psec	1 - 4 eV by frequency doubling	~10^8Hz	~10nJ
(d)	Dye Laser Pumped by modelocked cw Ar^+	≳1psec	1-2.3 eV	~10 Hz	~1nJ
(e)	Dye Laser Passively modelocked and pumped by cw Ar^+	≳0.1psec	2 eV	~10^8Hz	≲1nJ

Figure Captions

FIG 1 The polariton dispersion curves (solid curves) of CdS as compared with the uncoupled dispersion curves of the photon (dot-slashed curve), transverse exciton (broken curve) and longitudinal exciton (solid circles).

FIG 2 Schematic diagram showing the thermalization procedures for an optically excited exciton population.

FIG 3 (a) An example of how the temperature of a thermalized exciton population can be determined by fitting the lineshape of the phonon-assisted exciton recombination peak using Eq. (5). The solid line is the experimental luminescence spectrum of Cu_2O while the dots are calculated from Eq. (5) with $T = 7^{o}K$.

(b) An example of a nonthermalized emission spectra. The dots have been calculated from Eq. (5) with $T = 20^{o}K$ although the sample temperature was identical to (a). The crosses are theoretical results based on a nonthermal equilibrium exciton distribution. This figure is reproduced from Ref. 9.

FIG 4 A schematic diagram of the processes producing nonthermalized luminescence of excitons via phonon-assisted absorption and emission.

FIG 5 Exciton-phonon scattering rates in AgBr as determined from the time decay of the nonthermalized luminescence. This figure is reproduced from Ref. 22.

FIG 6 The theoretical and experimental TRPL spectra of the 1s exciton in Cu_2O. (a) and (c) are the theoretically computed exciton distributions as a function of time. (b) and (d) are the corresponding experimental distribution as determined from the Γ_{12}^{-} -phonon assisted recombination peak.

FIG 7 Theoretical decay rates of polaritons in CdS plotted as a function of polariton energies. The broken curve shows the radiative decay rates; the dotted curve is the phonon scattering rate, and the solid curve is the total decay rate.

FIG 8 A comparison between the calculated polariton decay time as obtained from the inverse of the polariton decay rate (solid curves) and the decay time determined by fitting the time-dependent polariton population with Eq. (4). (a) and (b) correspond to lattice temperatures of 0 and 25°K, respectively.

FIG 9 Theoretical polariton distribution function in CdS plotted at various time delays after excitation by a short optical pulse. The lattice temperature is assumed to be 10°K.

FIG 10 Schematic diagram of an experimental setup for performing time-resolved photoluminescence measurements using a delayed coincidence photon counting system.

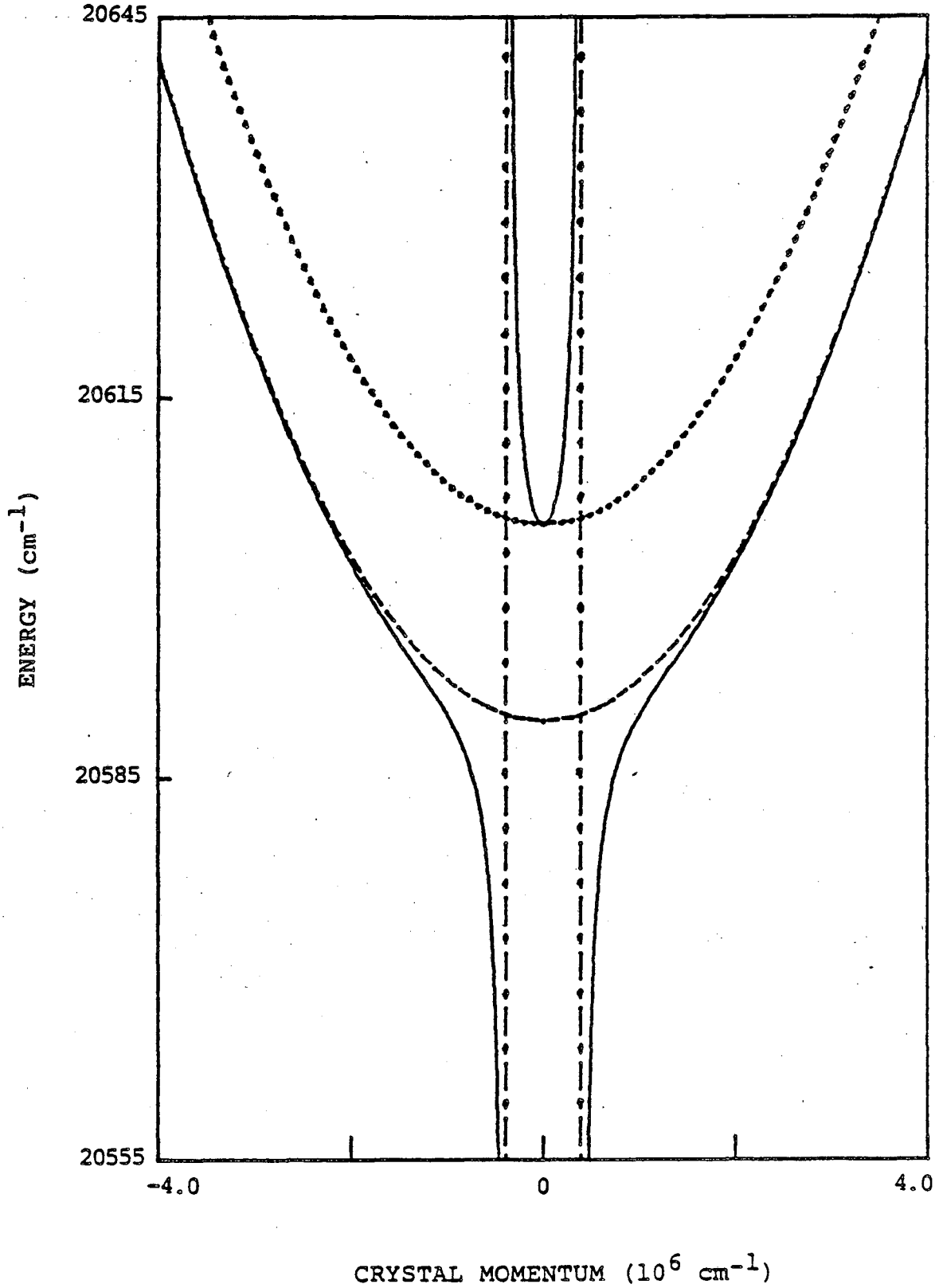
20645
20615
20585
20555
ENERGY (cm^{-1})
-4.0
0
4.0
CRYSTAL MOMENTUM (10^6 cm^{-1})

FIGURE 1

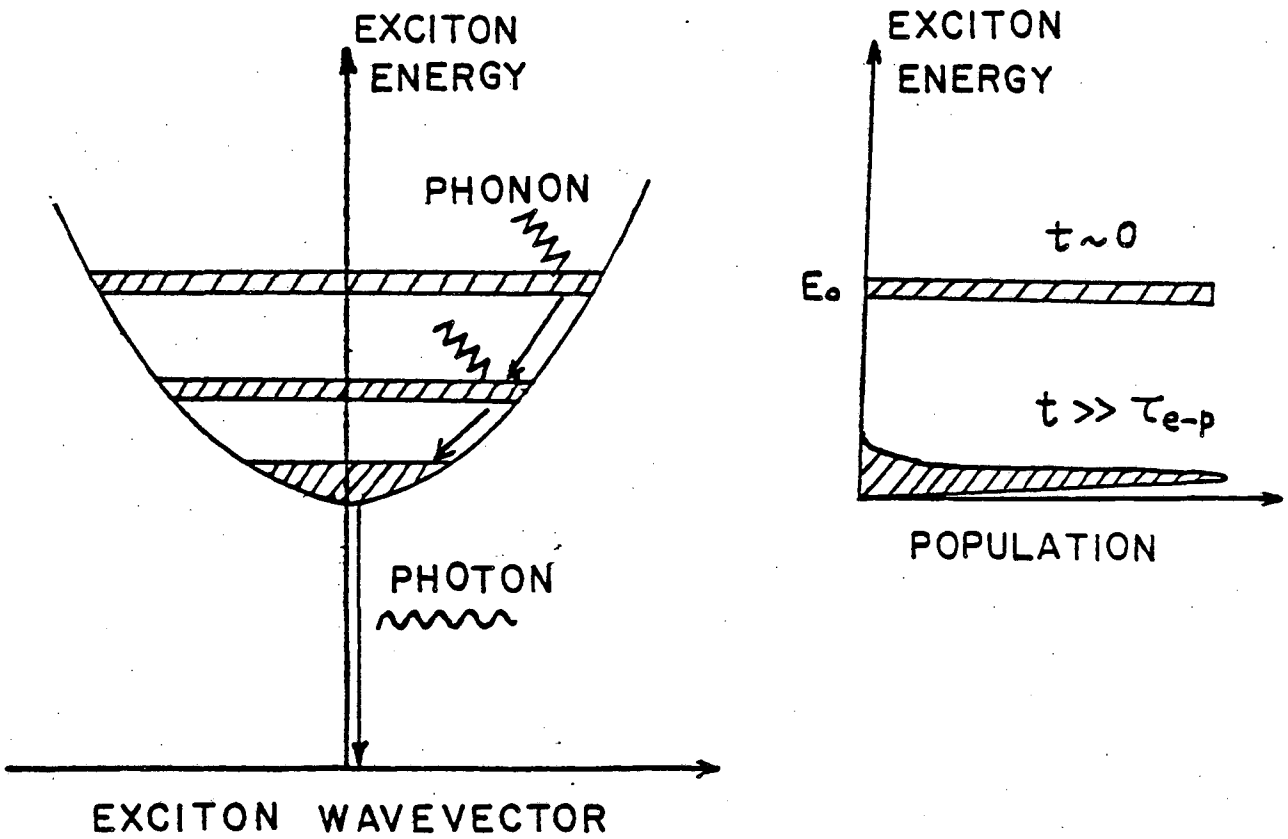
EXCITON
ENERGY
PHONON
PHOTON
EXCITON WAVEVECTOR
EXCITON
ENERGY
t ~ 0
E₀
t >> τe-p
POPULATION

FIGURE 2

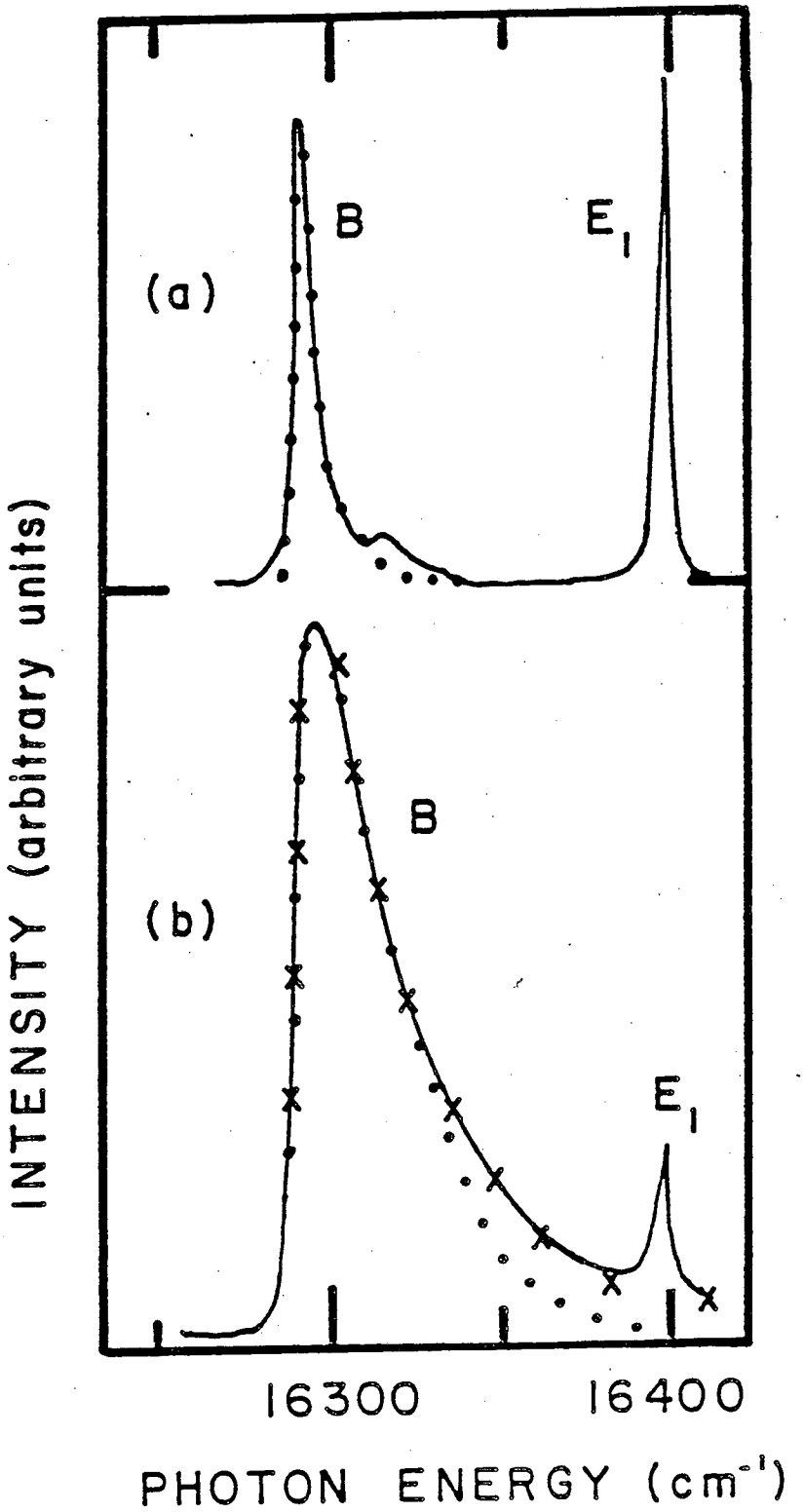
(a)
B
E1
(b)
B
E1
INTENSITY (arbitrary units)
16300
16400
PHOTON ENERGY (cm⁻¹)

FIGURE 3

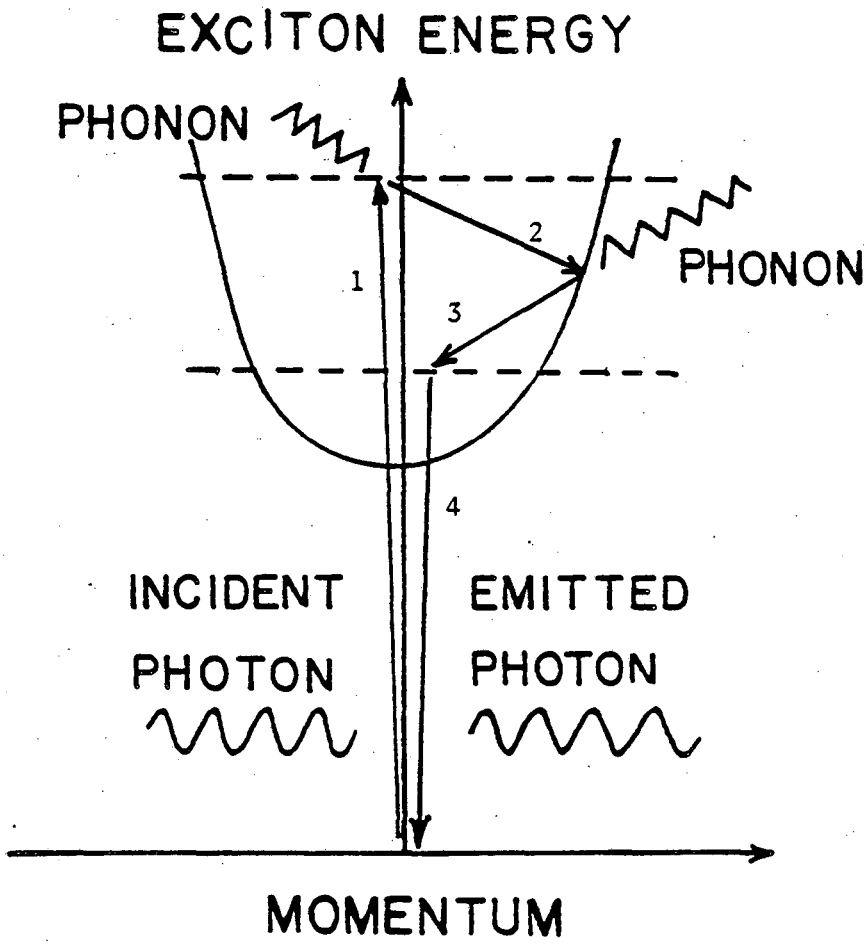
EXCITON ENERGY
PHONON
PHONON
1
2
3
4
INCIDENT
PHOTON
EMITTED
PHOTON
MOMENTUM

FIGURE 4

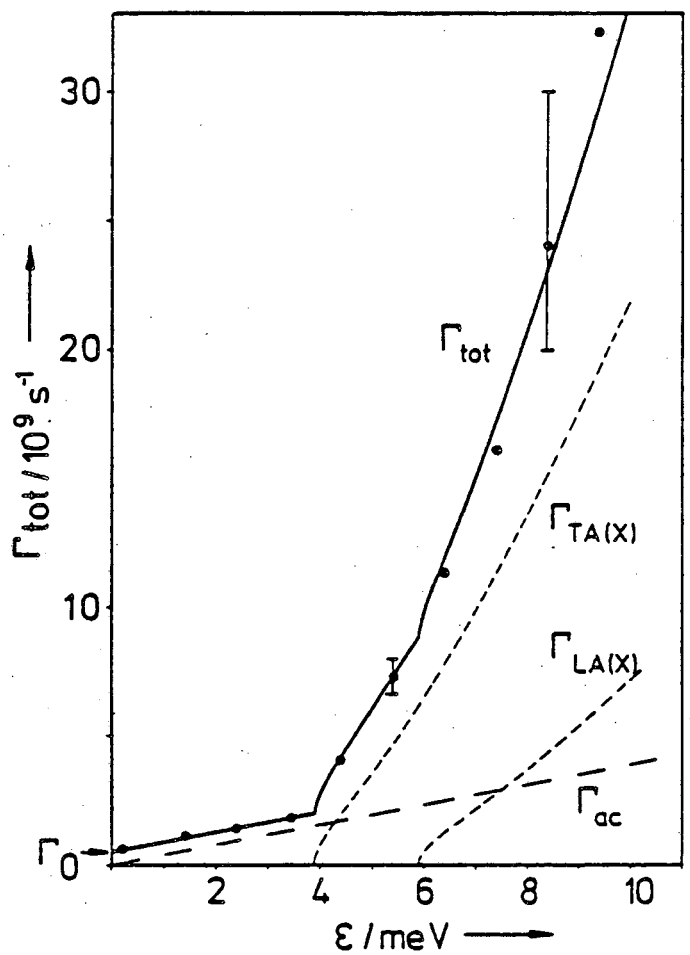
30
20
10
Γ_0
2
4
6
8
10
Γ_{tot}
$\Gamma_{TA(X)}$
$\Gamma_{LA(X)}$
Γ_{ac}
Γ_{tot} / 10^9 s^{-1}
ε / meV

FIGURE 5

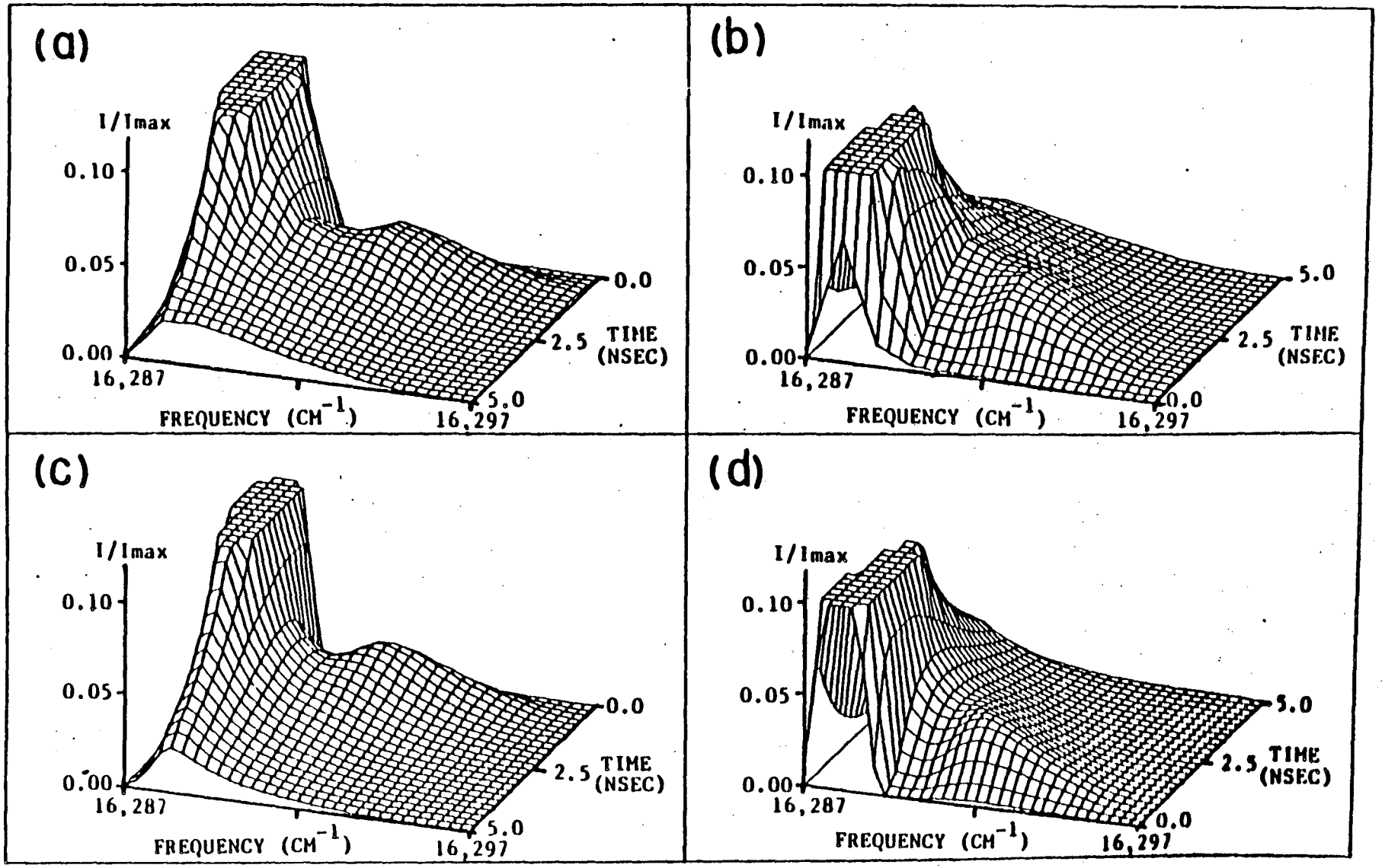

Figure 6

XBL 841-139

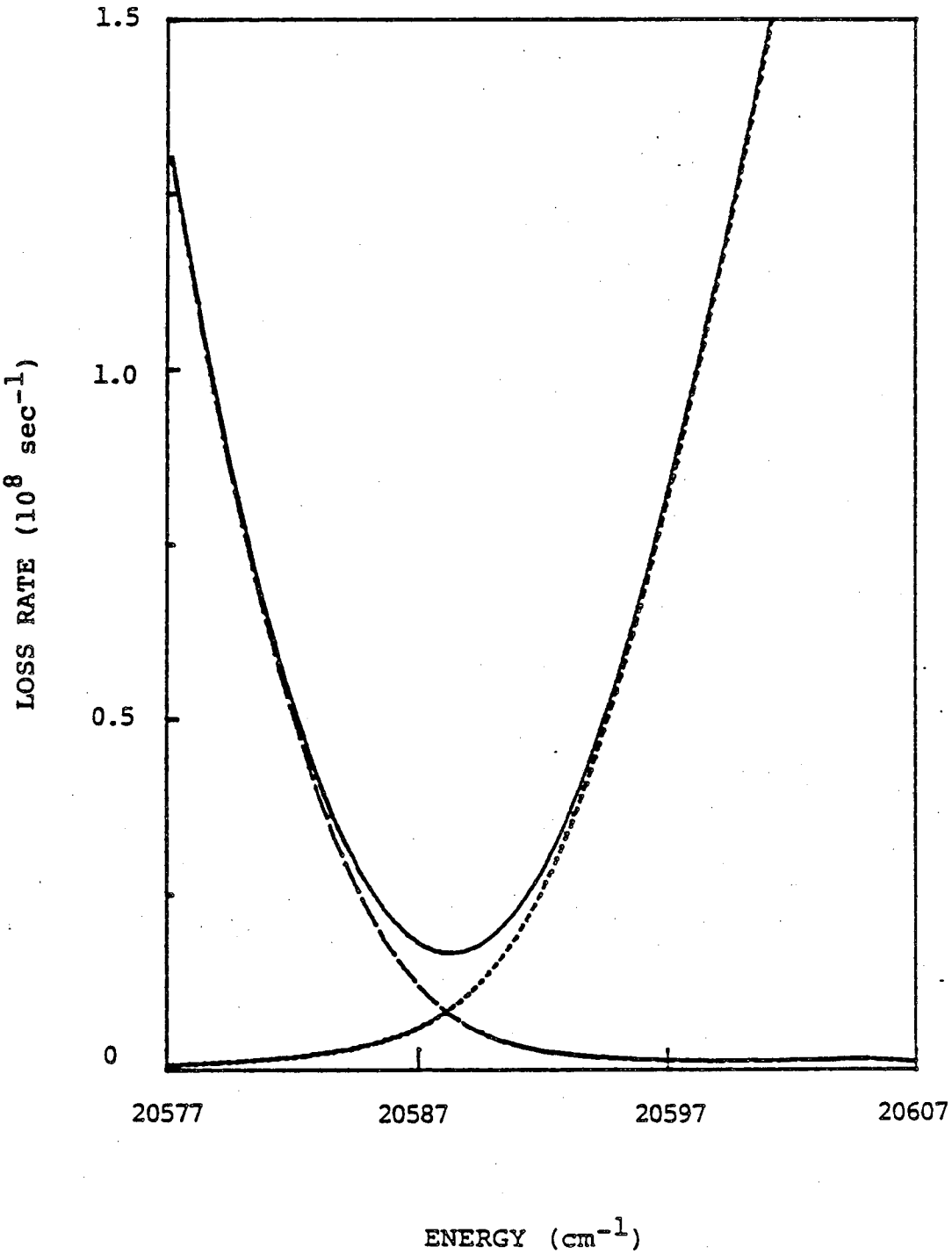
1.5
1.0
0.5
0
LOSS RATE (10^8 sec^{-1})
20577
20587
20597
20607
ENERGY (cm^{-1})

FIGURE 7

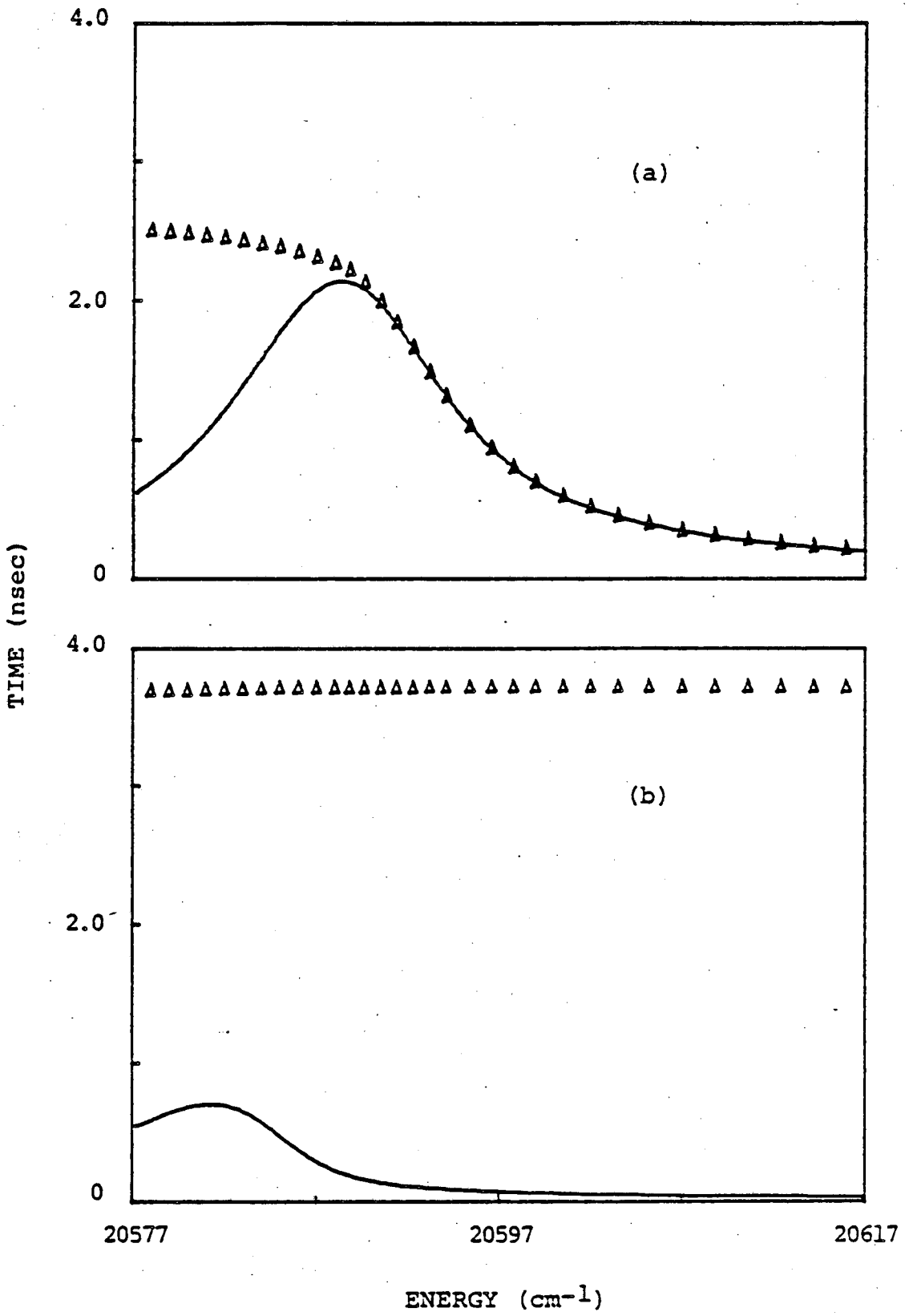

FIGURE 8

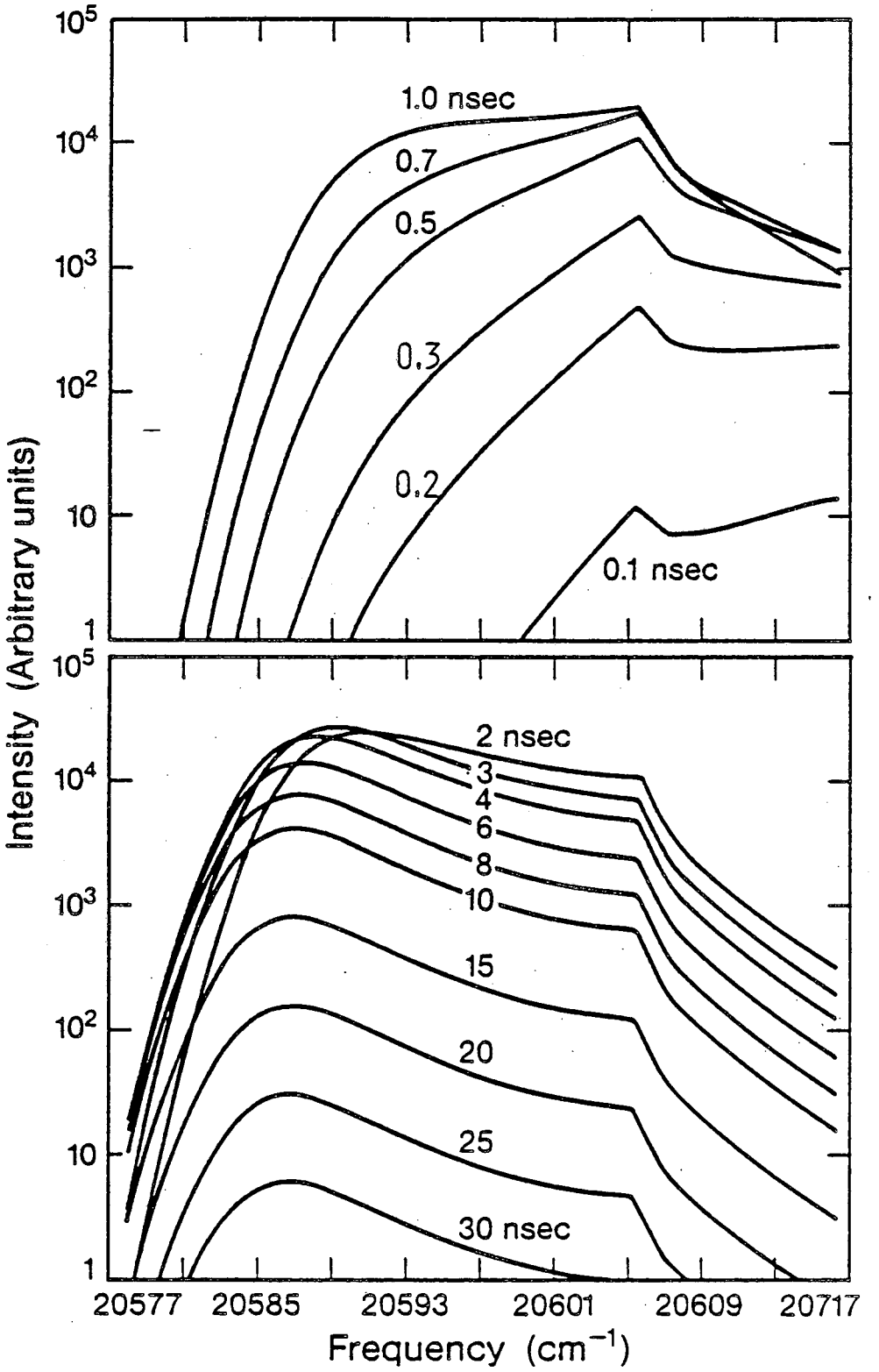
1.0 nsec
0.7
0.5
0.3
0.2
0.1 nsec
2 nsec
3
4
6
8
10
15
20
25
30 nsec
Intensity (Arbitrary units)
Frequency (cm^{-1})
20577
20585
20593
20601
20609
20717

FIGURE 9

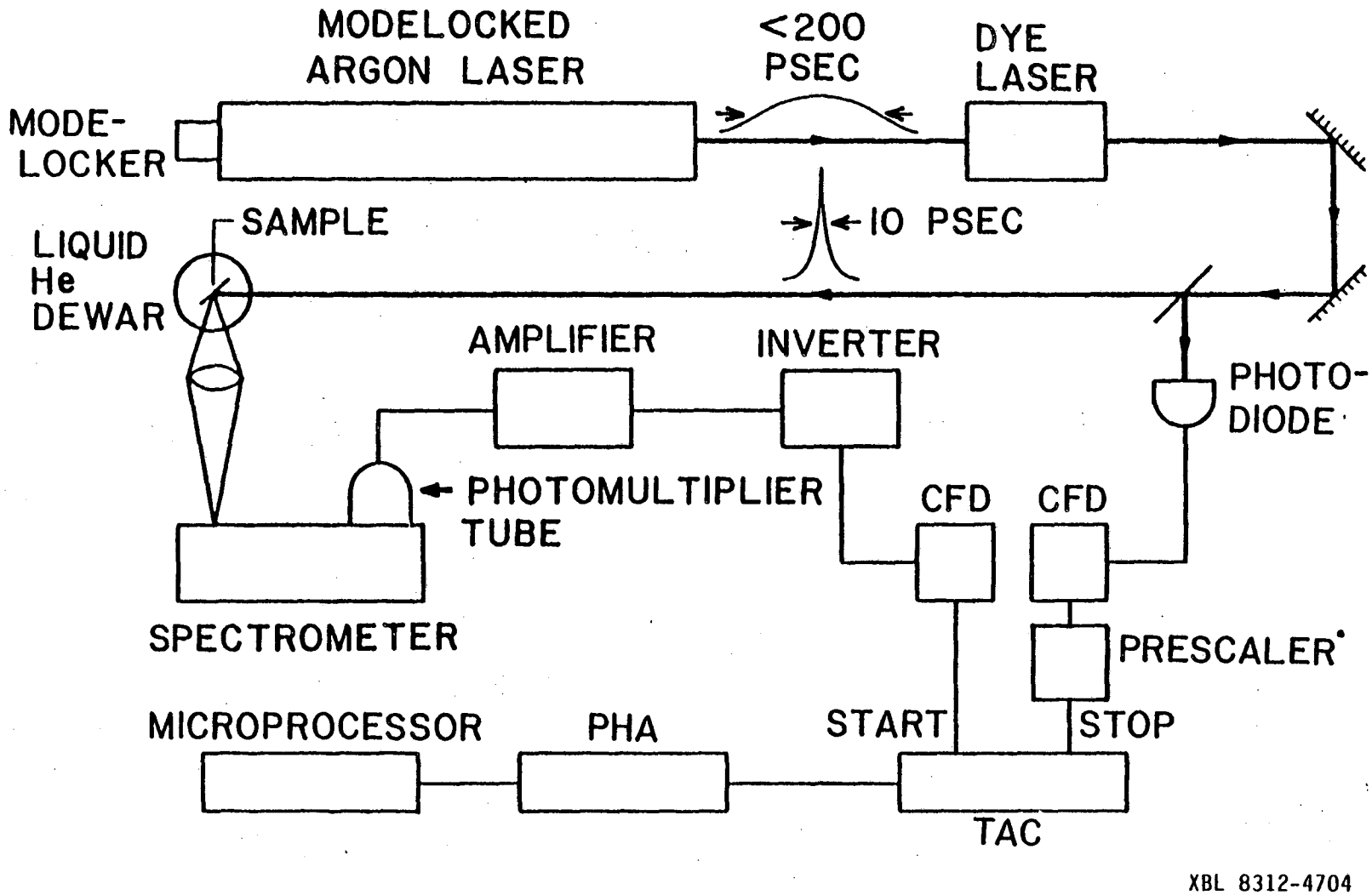
MODELOCKED
ARGON LASER
<200
PSEC
DYE
LASER
MODE-
LOCKER
10 PSEC
SAMPLE
LIQUID
He
DEWAR
AMPLIFIER
INVERTER
PHOTO-
DIODE
PHOTOMULTIPLIER
TUBE
CFD
CFD
SPECTROMETER
PRESCALER
MICROPROCESSOR
PHA
START
STOP
TAC
XBL 8312-4704

FIGURE 10

This report was done with support from the Department of Energy. Any conclusions or opinions expressed in this report represent solely those of the author(s) and not necessarily those of The Regents of the University of California, the Lawrence Berkeley Laboratory or the Department of Energy.

Reference to a company or product name does not imply approval or recommendation of the product by the University of California or the U.S. Department of Energy to the exclusion of others that may be suitable.

LAWRENCE BERKELEY LABORATORY
TECHNICAL INFORMATION DEPARTMENT
UNIVERSITY OF CALIFORNIA
BERKELEY, CALIFORNIA 94720